Complete and incomplete fusion in the ^{9}Be + ^{181}Ta reaction

N. T. Zhang,[1] Y. D. Fang,[1,*] P. R. S. Gomes,[2] J. Lubian,[2] M. L. Liu,[1] X. H. Zhou,[1,†] G. S. Li,[1] J. G. Wang,[1] S. Guo,[1] Y. H. Qiang,[1] Y. H. Zhang,[1] D. R. Mendes Junior,[2] Y. Zheng,[1] X. G. Lei,[1] B. S. Gao,[1,3] Z. G. Wang,[1,3] K. L. Wang,[1,3] and X. F. He[1,3]

[1]*Institute of Modern Physics, Chinese Academy of Sciences, Lanzhou 730000, China*

[2]*Instituto de Física, Universidade Federal Fluminense, Avenida Litoranea s/n, Gragoatá, Niterói, Rio de Janeiro 24210-340, Brazil*

[3]*Graduate University of Chinese Academy of Sciences, Beijing 000049, China*

(Received 22 April 2014; published 29 August 2014)

Complete and incomplete fusion cross sections for the ^{9}Be + ^{181}Ta system were measured at near barrier energies, using the offline gamma ray spectroscopy method. The results were compared with coupled channel calculations that do not take into account the coupling of the breakup channel, using a double folding potential as bare potential. A complete fusion suppression of the order of 35% was found, at energies above the barrier, whereas the total fusion cross sections are in agreement with the calculations. The ratio between incomplete fusion and total fusion at energies above the Coulomb barrier was found to be $32 \pm 1\%$. At sub-barrier energies one observes some enhancement of total fusion cross section.

DOI: 10.1103/PhysRevC.90.024621 PACS number(s): 25.60.Pj, 25.60.Gc, 25.70.Hi, 25.70.Gh

I. INTRODUCTION

The investigation of fusion cross sections between heavy ions has been extensively performed over the last 40 years. It is well established that low lying collective inelastic excitations of the colliding nuclei may lead to huge sub-barrier fusion enhancement when compared to predictions of unidimensional barrier penetration models, especially when highly deformed nuclei fuse [1–6]. It is also well known that transfer reactions can be an important doorway to enhance sub-barrier fusion cross sections [7–9]. At energies not too much above the barrier, the couplings of fusion to bound states are not expected to be important (at least not for too heavy systems), and therefore fusion excitation functions at this energy regime are usually well described by unidimensional barrier penetration models. In several works, fusion data above the barrier were indeed used to derive the barrier parameters.

This situation may be quite different when weakly bound nuclei are involved in the reactions. These nuclei have low breakup energy threshold and the breakup feeds states in the continuum. Apart from the usual direct compete fusion (DCF) of the whole projectile and target nuclei, other reaction mechanisms leading to fusion may occur, after the projectile or the target breaks into two or more fragments. Usually, the weakly bound nucleus is the projectile, and consequently it may break. In these cases, if all fragments fuse with the target, the process is called sequential complete fusion (SCF). If some, but not all fragments of the projectile fuse, one says that this is an incomplete fusion (ICF) process. Complete fusion (CF) is the sum of the DCF and SCF. Total fusion (TF) is the sum of CF and ICF. Reactions with weakly bound nuclei, both stable and radioactive, have been intensively studied in recent years, and there are some comprehensive reviews on this subject [10–13].

Maybe the most basic question in this field is whether the breakup process enhances or hinders the fusion cross section. The answer to this question may depend on the energy regime (above or below the Coulomb barrier) and on different target mass regions. However, before one tries to answer this question, some very important points have to be made clear. The first one is whether the investigation is concerned with CF or TF. Most of the experiments on fusion cross sections of weakly bound nuclei are only able to measure TF, since the residues of CF and ICF are very similar. Furthermore, direct transfer cross section might be added to the TF, since usually the nuclei formed in direct transfer of nucleons are similar to those produced by the ICF processes of these light projectiles. To be able to measure CF cross sections, one has to identify and measure the cross sections of all individual evaporation channels, and this is usually done by using the gamma ray (online and/or offline) spectroscopy method, or, for some particular systems, by detecting alpha particles emitted in the decay of residual nuclei or delayed x rays emitted in the decay of residual nuclei by electron capture. When some evaporation channels can not be measured, one has to rely on evaporation codes such as PACE [14], for adding the percentage of the missing channels to the measured partial fusion cross section. If this is only a small part of the CF cross section, this procedure does not add too much uncertainty on the final fusion cross section. However, one finds in the literature some reported "experimental fusion cross sections" for which more than 30% of the "measured" cross section comes from theoretical predictions.

Another very basic point which has to be clear is the definition of the reference to which one may say that the fusion cross section is enhanced or suppressed due to the coupling between the elastic channel and the continuum states representing the breakup channel. In the calculations, if one uses double folding potentials with realistic densities of the colliding nuclei as the bare potential, the possible static effects of the weakly bound nuclei, characterized by a longer tail of the optical potential, are already taken into account [15],

*fangyd@impcas.ac.cn
†zxh@impcas.ac.cn

and so the differences between data and calculations show only the dynamic effects of the channels not included in the coupled channel scheme. These channels are usually the breakup and transfer channels.

Some measurements of fusion cross sections of the weakly bound ^{9}Be projectile on different targets have been reported. ^{9}Be has neutron breakup energy of 1.67 MeV, and has no bound excited state. The ^{8}Be nucleus formed after the ^{9}Be breakup is unstable and breaks up into two alpha particles. If one of those alpha particles fuses with the target, one calls this process the ICF of the ^{9}Be. For light targets such as ^{27}Al [16] and ^{64}Zn [17,18], only TF was measured. For heavier targets, CF was measured, and for some of them ICF was also measured. Those targets were ^{89}Y [19], ^{124}Sn [20], ^{144}Sm [21], ^{186}W [22], ^{208}Pb [23,24], and ^{209}Bi [25]. For all systems where CF was measured, some CF suppression was found at energies above the barrier, and some enhancement was found at sub-barrier energies when compared with coupled channel calculations that do not include the breakup channel. Since for some systems the suppression of CF cross section was found to correspond to the measured ICF, it is usually assumed that the breakup hinders the CF by an amount of cross section equivalent to the ICF. However, contrary to what was found [20,26–28] for the CF of another stable weakly bound projectile, ^{6}Li, for which a CF suppression of the order of 20% to 30% was observed for any target, for the CF of ^{9}Be the suppression was found to vary with target from 10% to 40% of the theoretical CF predictions [29,30], without any observed systematics related to the target charge or mass. The reason for this peculiar behavior is not clear.

In order to contribute to the investigation of the fusion of ^{9}Be, in the present work we report the precise measurement of CF and ICF for the $^{9}\mathrm{Be} + {}^{181}\mathrm{Ta}$ system, at energies from around 5% below the Coulomb barrier to 35% above the barrier. One-neutron transfer cross sections were also measured, but this process will not be discussed in the present paper. Since the evaporation residues (ERs) mainly populated in the $^{9}\mathrm{Be} + {}^{181}\mathrm{Ta}$ reaction are β active, with lifetimes such that most of the radiation activity could be measured after irradiation, the technique of offline γ-ray measurements has been adopted in the present work.

This paper is organized as follows: a description of the experimental procedure is given in Sec. II; the results for ER and fusion cross sections are presented in Sec. III. Comparison of the data with coupled channel (CC) calculations and with a benchmark curve are presented in Sec. IV. The conclusions drawn from the present study are given in the last section.

II. EXPERIMENTAL PROCEDURE

The present experiment has been carried out using a collimated ^{9}Be beam with an initial energy of 50.4 MeV, delivered by the Heavy Ion Research Facility in Lanzhou (HIRFL), China. Two stacks of ^{181}Ta (99% enriched) targets having thicknesses in the range of 430–590 μg/cm^2 were irradiated in two individual runs. Each stack was composed of eight ^{181}Ta foils backed with Al foils of 0.92–1.07 mg/cm^2 thick and prepared by high vacuum evaporation technique at the China Institute of Atomic Energy (CIAE), Beijing. These Al foils were thick enough to completely stop all the evaporation residues and allowed reducing the energy of the beam on the subsequent targets and ensured a relatively wide energy range for measuring the excitation functions. Two Si (Au) surface-barrier detectors, at angles of $\pm 30^{0}$ with respect to the beam direction, were used to detect the elastically scattered particles from an Au foil placed upstream from our target stack.

According to the half-life of the main isotopes produced during irradiation, each stack was irradiated for about thirteen hours by the ^{9}Be beam. In the first run, the energy of the ^{9}Be ions falling on the first target in the stack was 50.3 MeV, determined by both the Rutherford scattering method using Si detectors and ATIMA calculation within the LISE++ program [31,32]. The projectile energy on each target foil has been estimated by calculating the energy loss in the target ^{181}Ta and catcher foil. Finally, the actual bombarding energy range of 42.3–50.3 MeV, in steps of 1.1–1.2 MeV, was exploited. In the second run, the same initial beam energy was used and a relatively thick Al foil (11.1 mg/cm^2) was placed in front of the target in order to obtain the acquired beam energy. This enabled us to obtain the irradiation at beam energies of 31.2–40.3 MeV, which were less than those in the first run of experiment. The typical ^{9}Be beam current throughout the experiment was about 20 e nA. The beam flux was calculated by the total charge measured in the Faraday cup installed after the target, while a negative 400 V bias on the collector repelled the secondary electrons.

One dedicated high-purity germanium (HPGe) array coupled to a Versa Module Europa (VME)-based data acquisition system (DAQ) has been developed to measure the induced activity in the target-catcher assembly. There were eight detector groups in this array, which could detect the gamma rays independently. Each group consisted of two HPGe detectors in a face-to-face geometry, where single γ-ray measurement and γ-γ coincidence measurement could be made simultaneously. One height-adjustable target holder was designed and placed at equal distance ($\sim$10 cm) from the two detectors in one group. This setup allowed measuring all the irradiated targets in one stack at a time. A thick Pb shield was inserted between two detector groups to reduce scattered gamma rays from neighboring targets and background from natural radioactivity. Three standard radioactive sources ^{60}Co, ^{133}Ba, and ^{152}Eu were used for the energy calibration as well as for the efficiency measurement. The gamma ray sources and the targets were counted in the same geometry and absorption conditions. The activity of each product was obtained from the measured counting rates using the known detector efficiency and published γ-ray branching ratios [33,34].

The fusion of ^{9}Be with ^{181}Ta forms the compound nucleus ^{190}Ir in an excited state which then decays predominantly by neutron evaporation to lower-A isotopes of Ir. None of these isotopes are stable and they decay mainly by electron capture. The γ rays from these ERs have been identified in the current experimental setup. Figures 1(a) and 1(b) show the typical offline γ-ray spectra from ERs following CF and ICF processes, respectively. In Fig. 1(b), the labels $\alpha 2n$ and $\alpha 3n$ correspond to the ERs when α fragment of the projectile produced in the breakup of ^{9}Be (in case of ICF), fuses with

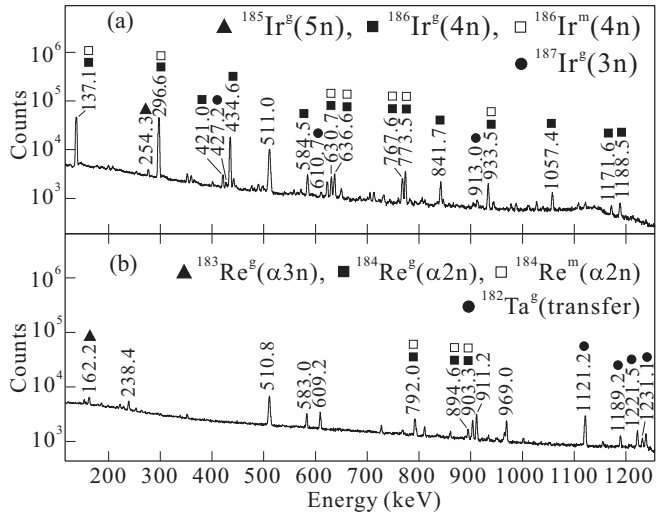

FIG. 1. Typical γ-ray spectra obtained from offline measurement at the projectile energy of 44.7 MeV after 4 h (a) and 54 d (b) of irradiation of the ^{181}Ta target with measuring times 1 h and 32 h, respectively. The 238.4, 583.0, 609.2, and 969.0 keV γ peaks come from natural background radiation.

the target and then evaporates $1n$ and $2n$, respectively. The unmeasured ERs were ^{186}Os ($p3n$ evaporation) and ^{187}Os ($p2n$ evaporation), which are stable and thus could not be measured using the offline counting method. These ERs as well as ^{188}Ir ($2n$ evaporation), also not measured, are expected to have low cross sections (less than 2.5% of σ_{CF} as estimated from the statistical model code PACE [14] over the present beam energy range). For details of ERs, see Table I.

III. RESULTS AND DATA REDUCTION

For all the ERs, the offline γ ray spectroscopy technique has been used in the determination of their relative cross sections [35]. The experimental reaction cross section $\sigma_\gamma(E)$ for a particular reaction product has been computed using the following expression given in Ref. [19]:

$$\sigma_\gamma(E) = \frac{N_\gamma \lambda}{N_t \varepsilon_\gamma I_\gamma (1 - e^{-\lambda \Delta t}) K}, \quad (1)$$

where

$$K = \sum_{n=0}^{m} I_n(t)[e^{-\lambda(t_w + n\Delta t)} - e^{-\lambda(t_w + t_m + n\Delta t)}]. \quad (2)$$

In Eqs. (1) and (2), t_m is the time of the measurement, t_w the time waited between the end of irradiation and start of measurement; N_γ is the total number of counts in the respective γ peak observed in time t_m; λ is the decay constant of the ER; N_t is the total number of nuclei present in the target; ε_γ is the efficiency of the HPGe detector at the peak energy; I_γ is the intensity branching ratio of the γ line; Δt is the step size (1 second was adopted in the present work) in which the current was recorded in the DAQ; and $I_n(t)$ is the beam current at the respective time interval.

The cross sections of different ER channels have been obtained from the observed intensities of the γ lines as listed in Table I with branching ratios corresponding to both ground (g) and metastable (m) states of ERs. The intense γ lines were chosen to evaluate the cross sections. The other γ lines corresponding to the same ERs were also used to cross-check the accepted cross-section values. The results are given in Table II. Errors on the measured ER cross sections were estimated by taking into account errors in absolute intensity of the γ peak, target thickness (~3%), and efficiency of the HPGe detector (~5%). It can be seen that the errors are minimum (~5.4% for σ_{4n} at $E_{\rm lab} = 50.3$ MeV) for the highest beam energies and they increase as one goes down in energy to a maximum of ~44% (σ_{3n} at $E_{\rm lab} = 35.3$ MeV) at lower energy. This large error is mainly due to the statistical uncertainties since the cross section and the intensity branching ratio of the characteristic γ ray are both very low.

The relative contributions of measured cross sections for neutron evaporation channels to CF have been compared with statistical model calculations performed using the code PACE [14]. The l distribution obtained from the FRESCO [36] calculations was fed as an input at each energy to obtain the cross sections. The results of PACE calculations for the ratios of $\sigma_{xn}/\sigma_{\Sigma xn}$ ($x = 3,4,5$) with level density equal to $A/10$ (solid line) are shown in Fig. 2, which provide a good description of the present experimental data. According to the PACE calculation, it is found that the summed cross sections of $3n$, $4n$, and $5n$ channels are in the range of 97.7%–99.0% of CF for the ^{9}Be + ^{181}Ta reaction. Therefore, the missing ER contributions to the total CF are negligible and the sum of xn channels, i.e., $\sigma_{\Sigma xn}$ ($x = 3,4,5$), was used to approximate the CF cross sections in this work.

In the ICF process, the Re nuclei are formed via the capture of an α fragment by the target and subsequent emission of neutrons. The dominant ICF channels are found to be $\alpha 2n$ (^{184}Re) and $\alpha 3n$ (^{183}Re). The possible $\alpha 1n$ (^{185}Re) channel cross section calculated by the code PACE, at energies equal to 4/9 of the ^{9}Be beam energies, was found to be negligibly small. However, it should be mentioned that the yields of Re

TABLE I. List of evaporation residues identified in the present measurement along with their half-lives $T_{1/2}$, J^π, E_γ, and absolute intensities I_γ [33,34]. The intense γ rays (in bold) were chosen to evaluate the cross sections.

Residue	$T_{1/2}$	J^π	E_γ (keV)	I_γ (%)
^{185}Ir^{g}($5n$)	14.4 h	$5/2^-$	254.4	13.3
			1828.8	10.0
^{186}Ir^{g}($4n$)	16.6 h	5^+	137.2	41.0
			434.8	33.9
			1057.2	3.06
^{186}Ir^{m}($4n$)	1.9 h	2^-	**987.0**	10.0
^{187}Ir^{g}($3n$)	10.5 h	$3/2^+$	610.7	3.93
			977.5	3.14
^{183}Re^{g}($\alpha 3n$)	70.0 d	$5/2^+$	**162.0**	24.5
^{184}Re^{g}($\alpha 2n$)	35.4 d	3^-	792.1	37.5
			903.3	37.9
^{184}Re^{m}($\alpha 2n$)	169.0 d	8^+	**216.0**	12.2
			920.9	8.14

TABLE II. Experimentally measured cross sections for all CF and ICF channels over the measured energy range.

E_{lab} (MeV)	^{185}Ir (mb)	^{186}Ir (mb)	^{187}Ir (mb)	^{183}Re (mb)	^{184}Re (mb)	σ_{CF} (mb)	σ_{ICF} (mb)
50.3	192.9 ± 12.7	400.5 ± 21.6	26.2 ± 5.8	196.6 ± 14.3	84.7 ± 5.6	619.6 ± 25.7	281.3 ± 15.4
49.2	139.4 ± 9.4	422.6 ± 28.1	29.6 ± 9.6	165.2 ± 13.0	89.8 ± 5.4	591.7 ± 31.1	255.0 ± 14.1
48.1	95.3 ± 7.0	461.5 ± 31.0	34.8 ± 12.2	156.3 ± 12.7	108.2 ± 15.0	591.6 ± 34.0	264.5 ± 19.7
47.0	46.4 ± 4.3	444.0 ± 24.6	38.3 ± 9.9	132.5 ± 7.9	109.7 ± 4.8	528.6 ± 26.9	242.2 ± 9.2
45.9	28.4 ± 4.5	421.0 ± 26.2	53.1 ± 9.4	114.9 ± 13.7	116.4 ± 19.1	502.4 ± 28.2	231.3 ± 23.5
44.7	7.6 ± 1.5	345.5 ± 21.8	56.1 ± 12.0	91.6 ± 7.1	112.2 ± 13.1	409.2 ± 24.9	203.8 ± 14.9
43.5	3.4 ± 1.4	258.6 ± 12.5	62.2 ± 12.8	55.9 ± 3.1	112.9 ± 6.6	324.2 ± 18.0	168.9 ± 7.3
42.3		207.6 ± 9.4	72.2 ± 12.3	36.4 ± 2.0	117.3 ± 5.6	279.7 ± 15.5	153.6 ± 5.9
40.3		115.4 ± 6.9	58.5 ± 8.1	15.9 ± 1.0	96.7 ± 6.1	173.9 ± 10.6	112.6 ± 6.2
39.0		60.8 ± 5.7	50.7 ± 9.0	7.8 ± 1.4	76.7 ± 4.6	111.5 ± 10.6	84.5 ± 4.8
37.8		23.1 ± 4.2	43.2 ± 7.2	5.2 ± 0.7	56.7 ± 3.6	66.2 ± 8.4	61.9 ± 3.7
36.5		5.8 ± 1.0	26.9 ± 5.9	2.6 ± 0.9	36.2 ± 3.3	32.7 ± 6.0	38.8 ± 3.4
35.3			12.7 ± 5.5	0.8 ± 0.2	9.7 ± 1.7	12.7 ± 5.5	10.6 ± 1.7

isotopes are not only ICF but the sum of ICF plus a possible contribution from the direct transfer reactions such as ^{4}He, ^{5}He and sequential one-neutron followed by alpha transfer from ^{8}Be; it is not possible experimentally to distinguish the ICF from the transfer reactions in the present experimental setup. Since the half-lives of ^{183}Re^{g} ($\alpha 3n$) and ^{184}Re^{g,m} ($\alpha 2n$) are much longer than the CF products, the measurements of ICF products did not start until the irradiated samples were cooled for more than one month. By doing so, all the CF products decayed away and the ICF products could be determined without interference from the CF products. Table II shows the ICF cross sections, which are the sum of $\sigma(^{183}\mathrm{Re})$ and $\sigma(^{184}\mathrm{Re})$. It is worth mentioning that the ICF probability, defined as the ratio between ICF and TF cross section, shows a smooth increase with decreasing projectile energy, from 30% to 35% at the energy range from $1.3V_B$ to $1.09V_B$, as can be observed in Fig. 3. An average ratio of 0.32 ± 0.01 is found in this energy range. At lower energies the ICF/TF ratio increases, reaching a maximum of 54%. The increase of the ratio at lower energies is due to the large contribution of direct stripping transfer reactions. At sub-barrier energies transfer cross sections are larger than fusion cross sections, since they do not need to tunnel the barrier, and consequently what one calls ICF in this regime is, actually, transfer plus ICF, with predominance of the first. For this reason, we determine the average value of ICF/TF only for energies above the barrier, where ICF predominates largely over transfer channels.

These results are impressively similar to those obtained by Dasgupta *et al.* [23,24] for the ^{9}Be + ^{208}Pb system. In that work, CF and ICF were measured by the detection online and offline of alpha particles originated by the decay of the residual nuclei. Their energy range was from $0.90V_B$ to $1.30V_B$. At the higher energies, they obtained the ICF/TF ratio of 30%, and the ratio increases slowly and smoothly up to 39% at $E_{c.m.}/V_B = 1.09$. Those values are identical to the ones shown in Fig. 3 for our ^{9}Be + ^{181}Ta system. At $E_{c.m.}/V_B = 1.0$, their ratio was 55%, whereas in the present work it is 54%. For their lowest energy, $E_{c.m.}/V_B = 0.90$, the ratio ICF/TF was found

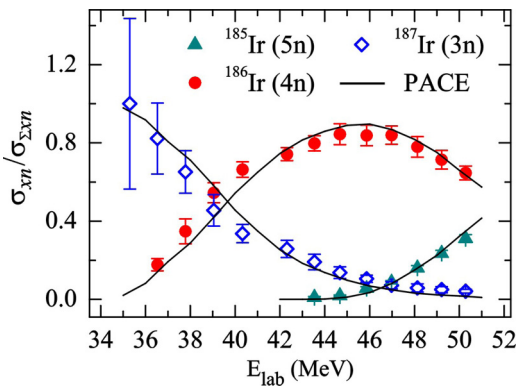

FIG. 2. (Color online) Experimental and predicted ratios of a given complete fusion xn evaporation product to the sum of all such products for the ^{9}Be + ^{181}Ta reaction.

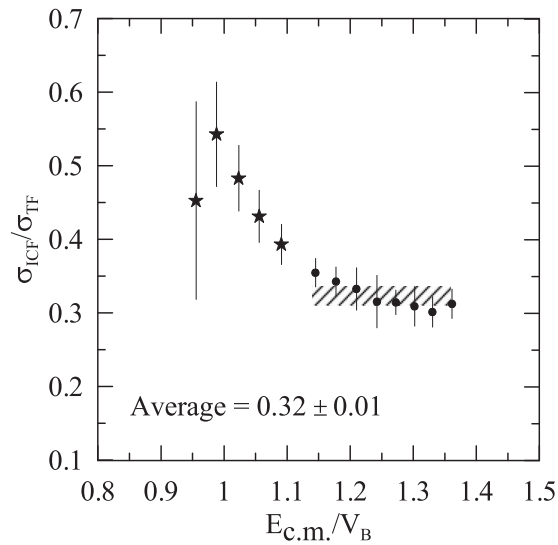

FIG. 3. Model independent ratio of ICF/TF. The mean ratio at energies above the Coulomb barrier is represented by a shadow region. The stars represent the points at energies below and near V_B, not taken into account to find the mean value of ICF/TF, while the full circles represent the points used to determine the mean value of the ratio at energies above V_B.

to be as high as 72%. So, in a model independent way, we verify that the ratio ICF/TF is the same for the ^{9}Be + ^{181}Ta, ^{208}Pb systems.

IV. COMPARISON OF DATA WITH THEORETICAL PREDICTIONS AND DISCUSSION

In this section we compare the measured CF and TF cross sections with the theoretical predictions of calculations that do not take into account the breakup and transfer processes. The bare potential used is the double folding Sao Paulo potential (SPP) [37], which uses realistic densities and has no free parameters. In the coupled channel calculations, we include only the inelastic excitations of the targets. No resonance in the continuum states of the ^{9}Be was included in the calculations, since this is already part of the breakup process. The ^{9}Be ground state deformation was not included. If we included this deformation, all results would change a little towards a larger theoretical value at sub-barrier energies. All coupled channel calculations were performed with the FRESCO code [36]. The imaginary part of the optical potential was taken internal to the barrier to account for the absorption of the flux that overcomes the Coulomb barrier. A Woods-Saxon form was used for this imaginary potential with parameters $W_0 = 50$ MeV, $r_0 = 1.06$ fm, and $a = 0.2$ fm for the depth, reduced radius, and diffuseness, respectively. The obtained cross sections were almost insensitive to changes of these parameters as long as the potential remained internal to the Coulomb barrier. In the coupled channels calculations, since the target is odd and assuming that the weak coupling approximation of the odd particle is valid, the coupled channel calculations were performed by considering the weak coupling of the $I^{\pi} = 7/2^{+}$ proton hole in the ^{182}W core with its ground state rotational band. The excitations of the core were considered up to the 6^{+} state at 0.6804 MeV. The quadrupole deformation parameters for the nuclear and Coulomb parts of the interaction were taken to be the same; they were obtained from Ref. [38] and are equal to $\beta_2 = 0.2508$.

The results of CC calculations are shown in Fig. 4. One can observe a CF suppression at energies above the barrier, and an agreement with the predictions at lower energies. Since realistic densities of the colliding nuclei were used, this effect corresponds to the dynamic effect of the breakup plus transfer channels, which were not included in the coupled channel scheme. On the other hand, one can also observe in Fig. 4 that the TF coincides with the theoretical predictions at energies above the barrier, and at sub-barrier energies one finds some TF enhancement.

Figure 5 is similar to Fig. 4, using the method proposed by Canto *et al.* [39]. In the vertical axis we plot the dimensionless function $\bar{F}(x)$, called renormalized fusion function, and in the horizontal axis we plot the energy variable x, defined as $\bar{F}_{\rm exp} = F_{\rm exp}\frac{F_0(x)}{F_{\rm CC}(x)}$ and $x = (E - V_B)/\hbar w$, where $F_i(x) = (2E_{\rm c.m.}/\pi R_B^2 \hbar\omega)\sigma_{{\rm fus},i}$ (subscript "i" stands for exp or CC) and V_B, R_B, and $\hbar w$ are the barrier height, radius, and the curvature of the Coulomb barrier. The full curve is the so-called universal fusion function (UFF) written as $F_0(x) = \ln[1 + \exp(2\pi x)]$, which is the benchmark curve. For this system, the barrier parameters extracted from the Sao Paulo potential are

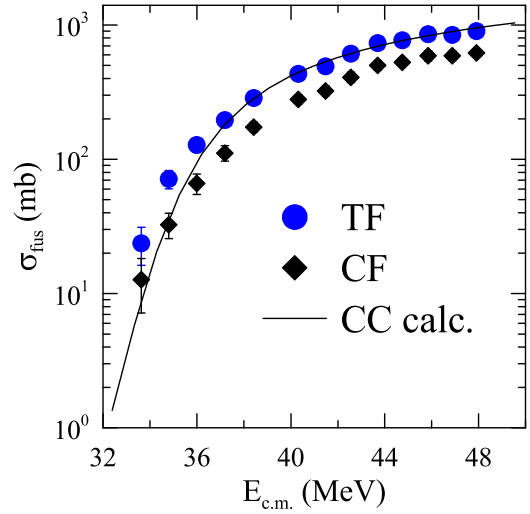

FIG. 4. (Color online) Experimental CF and TF excitation functions (points) and theoretical predictions using a parameter free folding potential as bare potential and CC calculations including target inelastic excitations (see text for details).

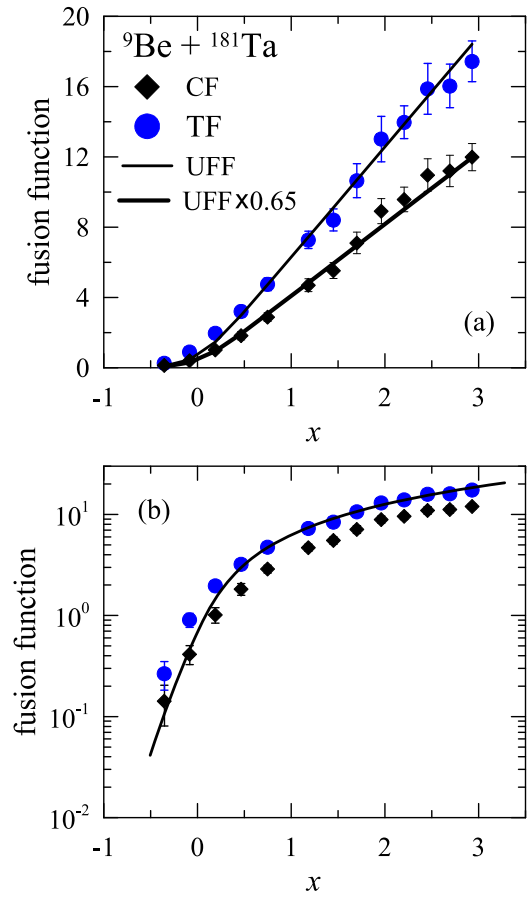

FIG. 5. (Color online) Renormalized experimental complete and total fusion functions versus the dimensionless energy variable x, following the prescription of Ref. [39]. $x = 0$ corresponds to the Coulomb barrier energy. The full curves are the universal fusion function (UFF) and the same curve multiplied buy the factor 0.65.

$V_B = 35.16$ MeV (in the center of mass), $R_B = 11.18$ fm, and $\hbar w = 4.35$ MeV. $x = 0$ corresponds to the barrier energy. The points are the experimental CF and TF functions, renormalized to take into account the effects of the couplings of inelastic excitations of the ^{181}Ta target, as explained in detail by Canto *et al.* [39]. The top [bottom] Fig. 5(a) [5(b)] is in linear [logarithmic] scale, which is suitable to observe the effects at energies above [below] the Coulomb barrier. The difference between the points and the UFF curve is the observed effect of the breakup of ^{9}Be on the CF and TF of the ^{9}Be $+ ^{181}$Ta system. To be more precise, this is the combined effect of breakup plus transfer channels. We can observe that the renormalized CF function coincides with the reference curve UFF when we multiply this curve by 0.65, corresponding to a suppression of 35% at energies above the barrier. The renormalized TF function, on the other hand, coincides with the UFF curve.

Gomes *et al.* [40] proposed an explanation to the different behaviors of the CF excitation function above and below the Coulomb barrier (suppression and enhancement), in terms of polarization potentials. They claim that at energies above the barrier the effect of breakup coupling, which produces a repulsive polarization potential, predominates over the effect of transfer channels, which produces an attractive polarization potential. At sub-barrier energies, the attractive polarization potential produced by transfer couplings predominates. As consequence, CF is suppressed at energies above the barrier and enhanced at sub-barrier energies, owing to the combined breakup and transfer couplings. From the present results, one may observe the predominance of breakup coupling effects at energies above the barrier, but similar importance of both channels at energies below the barrier, since in this energy regime the measured CF cross section coincides with the calculations. Indeed, Rafiei *et al.* [41] have shown, in a very precise and exclusive experiment, that at sub-barrier energies the transfer of one neutron followed by the breakup of ^{8}Be in its ground state predominates over the breakup of ^{9}Be into $^8\mathrm{Be} + n$, leaving the ^{8}Be in excited states.

As stated in the previous section, the CF suppression for the ^{9}Be $+ ^{181}$Ta, ^{208}Pb systems is almost the same within the experimental uncertainties. At a first sight, it may look strange that the CF suppression due to the breakup of ^{9}Be is nearly target independent, since one believes that the breakup probability increases with the target charge, owing to the stronger Coulomb field. Actually, Otomar *et al.* [42] and Hussein *et al.* [43] have shown recently that the nuclear breakup of the weakly bound ^{6}Li nucleus increases linearly with $A_T^{1/3}$ whereas the Coulomb breakup increases linearly with Z_T, for the same $E_{c.m.}/V_B$ energy, where A_T and Z_T are the mass and charge numbers of the target. However, as pointed out by the Australian National University (ANU) group in recent papers [41,44,45], two types of breakup must be considered: the prompt breakup which occurs when the projectile is close to and approaching the target and the delayed breakup, which occurs at large distances, when the projectile is already leaving the target region. Only the prompt breakup produces ICF and hence may affect the CF cross section. In Fig. 3 of Ref. [44] this is clearly shown. In one of those ANU papers, Rafiei *et al.* [41] reported the experiment where they measured sub-barrier breakup of ^{9}Be on different heavy targets. They were able to disentangle prompt and delayed breakups by combining Q value and relative energy of the fragments. They concluded that the delayed breakup of ^{8}Be, following the one-neutron transfer from ^{9}Be, has a lifetime of the order of 10^{-16} seconds and is ten times more intense than the prompt ^{9}Be breakup, which occurs within 10^{-22} seconds. Since the delayed breakup cannot affect fusion processes nor produce ICF, one cannot expect that the whole breakup process, for which the cross section increases with the target mass and/or charge, should have a simple relation to the fusion suppression. Those results are also in agreement with the ones by Hinde *et al.* [46] for the breakup of ^{9}Be. All those conclusions from the ANU group explain our present results.

V. SUMMARY AND CONCLUSIONS

We have measured the complete and incomplete fusion of the ^{9}Be $+ ^{181}$Ta system at near barrier energies, using the offline gamma ray spectroscopy method. Comparison of data with theoretical predictions from coupled channel calculations, without the inclusion of breakup and transfer channels, shows a CF suppression of around 35% at energies above the barrier and agreement at energies below the barrier. The TF excitation function is in agreement with the predictions at energies above the barrier, indicating that the suppression of the CF corresponds to the flux of events that produces the measured ICF of one alpha particle with the target, which is, on average, $32 \pm 1\%$. The same results were obtained by Dasgupta *et al.* [23,24] for the ^{208}Pb target, using a different experimental method to measure fusion cross sections. The combined results of the present work and the one by Dasgupta *et al.* show that the ratio ICF/TF and the CF suppression at energies slightly above the Coulomb barrier are similar and do not change, at least within a relatively small change of the target charge (73–82). The explanation for this behavior is that most of the ^{9}Be breakup is of the delayed type, which does not affect the fusion process. It would be interesting to measure the ICF/TF ratio for other systems nearly in the same charge region to confirm this conclusion. It would be also very interesting to check whether this conclusion holds for much lighter systems, if it is possible to separate ICF and CF for such light systems. In addition, the combined results of both works show that the two experimental methods are very reliable for the measurement of fusion cross sections.

ACKNOWLEDGMENTS

The authors are grateful to the staff of HIRFL for the operation of the cyclotron and friendly collaboration during the experiment. This work was supported by the National Natural Sciences Foundation (Grants No. U1232124, No. 11305221), the Major State Basic Research Development Program of China (Grant No. 2013CB834403), and ADS Project No. 302 (Grant No. Y103010ADS) of the Chinese Academy of Sciences. P.R.S.G., J.L., and D.R.M.J. acknowledge partial support from CNPq, FAPERJ and from Pronex.

[1] R. G. Stokstad, Y. Eisen, S. Kaplanis, D. Pelte, U. Smilansky, and I. Tserruya, Phys. Rev. Lett. **41**, 465 (1978); Phys. Rev. C **21**, 2427 (1980).
[2] S. Gil *et al.*, Phys. Rev. Lett. **65**, 3100 (1990).
[3] P. R. S. Gomes *et al.*, Phys. Rev. C **49**, 245 (1994).
[4] J. R. Leigh *et al.*, Phys. Rev. C **52**, 3151 (1995).
[5] D. E. DiGregorio *et al.*, Phys. Lett. B **176**, 322 (1986); Phys. Rev. C **39**, 516 (1989).
[6] V. V. Sargsyan, G. G. Adamian, N. V. Antonenko, W. Scheid, C. J. Lin, and H. Q. Zhang, Phys. Rev. C **85**, 037602 (2012); **85**, 017603 (2012); V. V. Sargsyan, G. G. Adamian, N. V. Antonenko, W. Scheid, and H. Q. Zhang, *ibid.* **84**, 064614 (2011).
[7] C. H. Dasso *et al.*, Nucl. Phys. A **405**, 381 (1983); **407**, 221 (1983); Phys. Lett. B **183**, 141 (1987).
[8] M. Beckerman *et al.*, Phys. Rev. Lett. **45**, 1472 (1980); Rep. Prog. Phys. **51**, 1047 (1988).
[9] K. E. Rehm, Annu. Rev. Nucl. Part. Sci. **41**, 429 (1991).
[10] L. F. Canto, P. R. S. Gomes, R. Donangelo, and M. S. Hussein, Phys. Rep. **424**, 1 (2006).
[11] J. F. Liang and C. Signorini, Int. J. Mod. Phys. E **14**, 1121 (2005).
[12] N. Keeley, R. Raabe, N. Alamanos, and J. L. Sida, Prog. Part. Nucl. Sci. **59**, 579 (2007).
[13] B. B. Back, H. Eesbensen, C. L. Jiang, and K. E. Rehm, Rev. Mod. Phys. **86**, 317 (2014).
[14] A. Gavron, Phys. Rev. C **21**, 230 (1980).
[15] P. R. S. Gomes, L. F. Canto, J. Lubian, and M. S. Hussein, Phys. Lett. B **695**, 320 (2011).
[16] G. V. Martí *et al.*, Phys. Rev. C **71**, 027602 (2005).
[17] S. B. Moraes *et al.*, Phys. Rev. C **61**, 064608 (2000).
[18] P. R. S. Gomes *et al.*, Phys. Lett. B **601**, 20 (2004); Phys. Rev. C **71**, 034608 (2005).
[19] C. S. Palshetkar *et al.*, Phys. Rev. C **82**, 044608 (2010).
[20] V. V. Parkar *et al.*, Phys. Rev. C **82**, 054601 (2010).
[21] P. R. S. Gomes *et al.*, Phys. Lett. B **634**, 356 (2006); Phys. Rev. C **73**, 064606 (2006).
[22] Y. D. Fang *et al.*, Phys. Rev. C **87**, 024604 (2013).
[23] M. Dasgupta *et al.*, Phys. Rev. Lett. **82**, 1395 (1999).
[24] M. Dasgupta *et al.*, Phys. Rev. C **70**, 024606 (2004).
[25] M. Dasgupta, D. J. Hinde, S. L. Sheehy, and B. Bouriquet, Phys. Rev. C **81**, 024608 (2010).
[26] H. Kumawat *et al.*, Phys. Rev. C **86**, 024607 (2012).
[27] L. R. Gasques, D. J. Hinde, M. Dasgupta, A. Mukherjee, and R. G. Thomas, Phys. Rev. C **79**, 034605 (2009).
[28] M. K. Pradhan *et al.*, Phys. Rev. C **83**, 064606 (2011).
[29] P. R. S. Gomes, R. Linares, J. Lubian, C. C. Lopes, E. N. Cardozo, B. H. F. Pereira, and I. Padron, Phys. Rev. C **84**, 014615 (2011).
[30] V. Jha, V. V. Parkar, and S. Kailas, Phys. Rev. C **89**, 034605 (2014).
[31] G. Scheidenberger and H. Geissel, Nucl. Instrum. Methods B **135**, 25 (1998).
[32] D. Bazin, O. Tarasov, M. Lewitowicz, and O. Sorlin, Nucl. Instrum. Methods A **482**, 307 (2002).
[33] ENSDF-National Nuclear Data Center, BNL, USA, http://www.nndc.bnl.gov/ensdf/
[34] *Table of Isotopes*, 8th ed., edited by R. B. Firestone (Wiley, New York, 1996).
[35] P. R. S. Gomes and T. J. P. Penna, Nucl. Instrum. Methods Phys. Res. A **280**, 395 (1989).
[36] I. J. Thompson, Comput. Phys. Rep. **7**, 167 (1988).
[37] L. C. Chamon, D. Pereira, M. S. Hussein, M. A. Candido Ribeiro, and D. Galetti, Phys. Rev. Lett. **79**, 5218 (1997); Phys. Rev. C **66**, 014610 (2002).
[38] S. Raman, C. W. Nestor, Jr., and P. Tikkanem, At. Data Nucl. Data Tables **78**, 1 (2001).
[39] L. F. Canto *et al.*, J. Phys. G **36**, 015109 (2009); Nucl. Phys. A **821**, 51 (2009).
[40] P. R. S. Gomes *et al.*, J. Phys. G **39**, 115103 (2012).
[41] R. Rafiei, R. duRietz, D. H. Luong, D. J. Hinde, M. Dasgupta, M. Evers, and A. Diaz-Torres, Phys. Rev. C **81**, 024601 (2010).
[42] D. R. Otomar, P. R. S. Gomes, J. Lubian, L. F. Canto, and M. S. Hussein, Phys. Rev. C **87**, 014615 (2013).
[43] M. S. Hussein, P. R. S. Gomes, J. Lubian, D. R. Otomar, and L. F. Canto, Phys. Rev. C **88**, 047601 (2013).
[44] D. H. Luong *et al.*, Phys. Lett. B **695**, 105 (2011).
[45] D. H. Luong, M. Dasgupta, D. J. Hinde, R. duRietz, R. Rafiei, C. J. Lin, M. Evers, and A. Diaz-Torres, Phys. Rev. C **88**, 034609 (2013).
[46] D. J. Hinde, M. Dasgupta, B. R. Fulton, C. R. Morton, R. J. Wooliscroft, A. P. Berriman, and K. Hagino, Phys. Rev. Lett. **89**, 272701 (2002).